Available online at www.sciencedirect.com

SCIENCE DIRECT®

ELSEVIER

International Journal of Solids and Structures 42 (2005) 3093–3113

INTERNATIONAL JOURNAL OF SOLIDS and STRUCTURES

www.elsevier.com/locate/ijsolstr

Some problems in the antiplane shear deformation of bi-material wedges

A.R. Shahani *

Department of Applied Mechanics, Faculty of Mechanical Engineering, K.N.T. University of Technology, P.O. Box 016765-3381, Tehran, Iran

Received 19 October 2004; received in revised form 3 November 2004
Available online 19 December 2004

Abstract

The antiplane shear deformation of a bi-material wedge with finite radius is studied in this paper. Depending upon the boundary condition prescribed on the circular segment of the wedge, traction or displacement, two problems are analyzed. In each problem two different cases of boundary conditions on the radial edges of the composite wedge are considered. The radial boundary data are: traction–displacement and traction–traction. The solution of governing differential equations is accomplished by means of finite Mellin transforms. The closed form solutions are obtained for displacement and stress fields in the entire domain. The geometric singularities of stress fields are observed to be dependent on material property, in general. However, in the special case of equal apex angles in the traction–traction problem, this dependency ceases to exist and the geometric singularity shows dependency only upon the apex angle. A result which is in agreement with that cited in the literature for bi-material wedges with infinite radii. In part II of the paper, Antiplane shear deformation of bi-material circular media containing an interfacial edge crack is considered. As a special case of bi-material wedges studied in part I of the paper, explicit expressions are derived for the stress intensity factor at the tip of an edge crack lying at the interface of the bi-material media. It is seen that in general, the stress intensity factor is a function of material property. However, in special cases of traction–traction problem, i.e., similar materials and also equal apex angles, the stress intensity factor becomes independent of material property and the result coincides with the results in the literature.

* Corresponding author. Tel.: +98 217343300; fax: +98 217334338.
E-mail address: shahani@kntu.ac.ir

0020-7683/$ - see front matter
doi:10.1016/j.ijsolstr.2004.11.002

1. Introduction

Bonded wedges of different materials have been under consideration in the recent decades. Bogy (1971) and Dempsey and Sinclair (1979, 1981) studied the in-plane problem of two edge-bonded elastic wedges of different materials. Ma and Hour (1989) analyzed the antiplane shear deformation problem of simple isotropic, bi-material and anisotropic wedges with infinite radii. All of the above-mentioned papers were devoted to the analysis of the order of stress singularity at the wedge apex. In fact, the stress fields may have a form of the order $O(r^{-\lambda_s})$ near the apex ($r \rightarrow 0$), in which λ_s is called the order of stress singularity. Ting (1986) studied the order of stress singularity at the tip of an interface crack in a single isotropic and anisotropic material under in-plane loading. Indeed, the base of his studies was the in-plane problem of a simple wedge in special apex angles π and 2π. The antiplane shear deformation problem of isotropic as well as anisotropic finite wedges was solved under different boundary conditions by Kargarnovin et al. (1997) and Shahani (1999), respectively. Analytical solutions for the displacement and stress fields were derived and explicit expressions for the order of stress singularity at the wedge apex were extracted. Meanwhile, the conditions for which the stress singularity *does* occur at the apex were derived as functions of geometry and material property. In a recent paper (Shahani, submitted), the author have derived closed form relations for the stresses directly from the series form equations of Kargarnovin et al. (1997), using mathematical techniques. It has been shown that the $\tau_{\theta z}$-component is unbounded at the point of application of the concentrated tractions, however, the τ_{rz}-component is convergent at that point. Also, continuity of the τ_{rz}-component over the entire wedge is studied. The facts which were not apparent from the series form solutions of Kargarnovin et al. (1997). On the other hand, Fariborz (2004) has shown the continuity of the τ_{rz}-component of the paper Kargarnovin et al. (1997) along the arc $r = h$, numerically. Shahani and Adibnazari (2000) considered the antiplane shear deformation problem of perfectly bonded dissimilar wedges with infinite radii as well as bonded wedges with an interfacial crack. They extracted explicit expressions for the stress distribution in the bi-material wedge under traction–traction boundary conditions on the radial edges of the composite wedge and showed that in the special case of equal apex angles (but still with different materials), the stress distribution releases its dependency to the material property. In a recent paper, the author (Shahani (2001)) derived a closed form solution for an edge crack lying at the interface of two edge-bonded wedges and terminating to the apex.

The only paper which deals with the antiplane shear deformation of bi-material wedges with *finite* radius is that of Kargarnovin and Fariborz (2000). This work has been restricted to the derivation of the displacement field, near the wedge apex only. Meanwhile, only "the dominant solution for displacement field near the wedge apex has been obtained (Kargarnovin and Fariborz, 2000)".

The finiteness of the radius of the wedge causes that the effect of different possible boundary conditions on the circular segment of the wedge become important.

On the other hand, analytical expressions for the stress intensity factors of different geometries and various loadings are important in fracture mechanics. In the area of mode III problems, a number of contributions are related to the problem of finite or semi-infinite cracks in an infinite medium (Suo, 1989; Shiue et al., 1989; Choi et al., 1994; Lee and Earmme, 2000; Shahani and Adibnazari, 2000; Shahani, 2001). However, the interaction of finite boundaries on the cracks affects the severity of the induced stresses near the crack tip. Also, edge cracks vastly occur in composite laminates and bonded structures. Hence, edge delamination or edge debonding between the laminas or dissimilar components has appeared to become the main failure mode of these materials.

Most interfacial edge crack problems analyzed in the literature to date considered cracks between two bonded quarter planes. In a recent paper, the author (Shahani, 2003) has analyzed the antiplane shear deformation of several edge-cracked geometries and derived analytical expressions for the stress intensity factor of single-material circular shafts with edge cracks, bonded half planes containing an interfacial edge crack, bonded wedges with an interfacial edge crack terminating to the apex and also DCB's. All of the above-mentioned problems have been analyzed under traction–traction boundary conditions.

In the present paper, antiplane shear deformation of two dissimilar edge-bonded wedges with finite radii is studied. The paper is organized in two parts. In part I, stress and singularity analysis in bi-material finite wedges is considered. Two problems related to the type of boundary condition prescribed on the circular portion of the boundary are studied. The traction free and fixed displacement conditions are imposed on the arc for problems I and II, respectively. The boundary conditions on the radial edges of the composite wedge in these problems are: traction–displacement and traction–traction. The tractions are assumed to act concentrically which allows the solutions to be used as the Green's function for the analysis of a bi-material wedge under general distribution of traction. The solution is accomplished by employing the finite Mellin transforms. The full field solution is obtained for displacement and stresses. Also, analytical expressions are derived for the orders of stress singularity. In general, the order of stress singularity depends on the material property of the bi-material wedge. However, in special cases, the order of stress singularity releases its dependency to the material property, a fact which is in agreement with the published results in the literature. It is shown, as was expected, that in the special case of a bi-material wedge with infinite radius, the results of the two problems become identical.

In part II of the present paper, analytical expressions are derived for the stress intensity factors in different geometries of bi-material circular media containing an interfacial edge crack. Parallel to that followed in part I, the stress intensity factor expressions are extracted for problems I and II, i.e., traction-free and fixed displacement boundary conditions on the circular portion of the boundary, respectively. In fact, the finite boundary (finite radius of the bi-material circular media) affects the analytical expressions for the stress intensity factors. Furthermore, in each problem, two cases of boundary conditions corresponding to the boundary data prescribed on the crack faces are considered, which are: traction–displacement and traction–traction. As in part I of the paper, in all of the problems concentrated antiplane tractions are assumed to act which allows the solutions to be used as the Green's function for obtaining the stress intensity factor of any General distribution of tractions. Various combinations of the apex angles are considered for which closed form solutions are obtained for the related characteristic equations and explicit relations are derived for the stress intensity factor. Generally, the stress intensity factors are dependent on the material property (mismatch ratio of the composite wedge), however, in special cases of traction–traction problem, i.e., similar materials and also equal apex angles, the stress intensity factor becomes independent of material property and the obtained results coincide with the results in the literature. In addition, in the special case of infinite bi-material media with an interfacial edge crack, the stress intensity factors can easily be obtained by letting the radius of the circular media to approach infinity.

2. Part I: stress and singularity analysis in bi-material finite wedge

2.1. Formulation and problem solution

Consider two dissimilar isotropic wedges with finite radii, a, apex angles α and β, shear moduli μ_1, μ_2, and infinite lengths in the direction perpendicular to the plane of the wedge, which are bonded together along a common edge (Fig. 1). The common edge is chosen as the reference axis for defining the coordinate θ. The condition of antiplane shear deformation is imposed on the composite wedge. This implies that the only nonzero displacement component be the out of plane component, W_i, which is a function of the in-plane coordinates (r,θ). Therefore, the nonvanishing stress components are $\tau^i_{rz}(r,\theta)$, $\tau^i_{\theta z}(r,\theta)$. The subscript and superscripts, i, in the displacement and stress components indicate these functions in the ith wedge $(i = 1,2)$. The constitutive equations for isotropic materials undergoing antiplane deformation reduce to

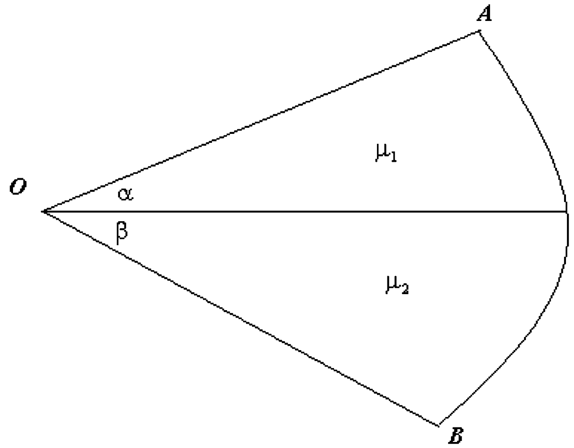

Fig. 1. Schematic view of a bi-material wedge.

$$\tau^i_{rz} = \mu_i \frac{\partial W_i}{\partial r} \quad \tau^i_{\theta z} = \frac{\mu_i}{r}\frac{\partial W_i}{\partial \theta}; \qquad i = 1,2 \tag{1}$$

In the absence of body forces, by making use of (1), the equilibrium equation in terms of displacement appears as

$$\frac{\partial^2 W_i}{\partial r^2} + \frac{1}{r}\frac{\partial W_i}{\partial r} + \frac{1}{r^2}\frac{\partial^2 W_i}{\partial \theta^2} = 0; \quad i = 1,2 \tag{2}$$

One piece of boundary data prevailing in all the cases treated in problem I is the traction-free condition on the circular segment of the wedge circumference

$$\tau^i_{rz}(a,\theta) = 0 \tag{3}$$

In problem II the wedge is fixed on the circular segment of the boundary. Thus

$$W_i(a,\theta) = 0 \tag{4}$$

The solution to the Laplace's equation (2) for a finite wedge may be accomplished by means of the finite Mellin transforms. The finite Mellin transform of first and second kinds are defined, respectively (Sneddon, 1972) as

$$\begin{aligned} M_1[W_i(r,\theta)] = W^*_{i1}(S,\theta) = \int_0^a \left(\frac{a^{2S}}{r^{S+1}} - r^{S-1}\right) W_i(r,\theta)\mathrm{d}r \\ M_2[W_i(r,\theta)] = W^*_{i2}(S,\theta) = \int_0^a \left(\frac{a^{2S}}{r^{S+1}} + r^{S-1}\right) W_i(r,\theta)\mathrm{d}r \end{aligned} \tag{5}$$

where S is a complex transform parameter. The inversions of these transforms are represented by (Kargarnovin et al., 1997)

$$M_j^{-1}[W^*_{ij}(S,\theta)] = W_i(r,\theta) = \frac{(-1)^j}{2\pi \mathrm{i}} \int_{c-\mathrm{i}\infty}^{c+\mathrm{i}\infty} r^{-S} W^*_{ij}(S,\theta)\mathrm{d}S \quad (i,j = 1,2) \tag{6}$$

It should be noted that the parameter, i, in the denominator and also in the limits of the integral is the so-called pure imaginary number $i = \sqrt{-1}$, and should not be confused with the sub/superscript parameter, i. Application of the Mellin transform of first kind in conjunction with integration by parts in (2) yields

$$\left(\frac{d^2}{d\theta^2}+S^2\right)W_{i1}^*(S,\theta)+2Sa^S W_i(a,\theta)=0; \quad (i=1,2) \tag{7}$$

provided that

$$\lim_{r\to 0}\left[(a^{2S}r^{-S}-r^S)r\frac{\partial W_i(r,\theta)}{\partial r}+S(a^{2S}r^{-S}+r^S)W_i(r,\theta)\right]=0 \tag{8}$$

Similarly, employing the Mellin transform of second kind in (2), leads to

$$\left(\frac{d^2}{d\theta^2}+S^2\right)W_{i2}^*(S,\theta)+2a^{S+1}\frac{\partial W_i(a,\theta)}{\partial r}=0 \quad (i=1,2) \tag{9}$$

provided that

$$\lim_{r\to 0}\left[(a^{2S}r^{-S}+r^S)r\frac{\partial W_i(r,\theta)}{\partial r}+S(a^{2S}r^{-S}-r^S)W_i(r,\theta)\right]=0 \tag{10}$$

The conditions expressed by (8) and (10) specify the strip of regularity which is the range of proper values for the real quantity C in the inversion formulas (6). Applying the boundary condition (4) in (7), and the boundary condition (3) with the aid of the first of (1) in (9) lead to the following equation for both problems:

$$\frac{d^2W_{ij}^*}{d\theta^2}+S^2W_{ij}^*=0 \quad (i,j=1,2) \tag{11}$$

The solution to this equation is readily known to be

$$W_{ij}^*(S,\theta)=A_i(S)\sin(S\theta)+B_i(S)\cos(S\theta) \quad (i,j=1,2) \tag{12}$$

In the following two problems the boundary data on the radial edges are enforced to compute the unknown coefficients in (12). The values of j are 2 and 1 in problems I and II, respectively.

2.2. Problem I

Two different cases are analyzed here, depending upon the boundary conditions applied on the radial edges of the composite wedge. If one of the edges is fixed and the other one is subjected to a concentrated traction, we have a traction–displacement problem. On the other hand, if both edges are subjected to concentrated tractions, which are of opposite direction, a traction–traction problem is encountered. These cases for problem I are analyzed separately in this section.

2.2.1. Case Ia—traction–displacement

The corresponding boundary conditions of the problem in this case are

$$\begin{aligned} &W_2(r,-\beta)=0\\ &\tau_{\theta z}^1(r,\alpha)=P\delta(r-h)\\ &W_1(r,0)=W_2(r,0)\\ &\tau_{\theta z}^1(r,0)=\tau_{\theta z}^2(r,0)\end{aligned} \tag{13}$$

where δ denotes the Dirac-delta function. It is worth-mentioning that the choice of the second of boundary conditions (13), leads to the Green's function solution for the problem. The latter two conditions correspond to the continuity of the displacement and tractions due to the perfect bonding. Applying the Mellin transform of second kind with the aid of the second of Eq. (1), if necessary, on the boundary conditions (13) and then, applying these transformed boundary conditions on Eq. (12) result in the unknown coefficients. The transformed displacements may then be obtained as

$$W_{12}^*(S,\theta) = \frac{P(a^{2S}h^{-S} + h^S)[R\sin(S\theta)\cos(S\beta) + \cos(S\theta)\sin(S\beta)]}{\mu_1 S[R\cos(S\alpha)\cos(S\beta) - \sin(S\alpha)\sin(S\beta)]}$$
$$W_{22}^*(S,\theta) = \frac{P(a^{2S}h^{-S} + h^S)\sin[S(\theta+\beta)]}{\mu_1 S[R\cos(S\alpha)\cos(S\beta) - \sin(S\alpha)\sin(S\beta)]} \tag{14}$$

where

$$R = \frac{\mu_2}{\mu_1} \tag{15}$$

The obtained transformed displacements are meromorphic functions of S. The displacement functions in the two wedges can be obtained by applying the inverse Mellin transform, Eq. (6), with $j = 2$ in Eq. (14). The resultant complex integrals should be computed using the residue theorem. The procedure of these contour integrations have been completely outlined by Kargarnovin et al. (1997) and are omitted here for the sake of brevity. The full field displacement functions may then be obtained as follows:

$$W_1(r,\theta) = \frac{P}{\mu_1(R\alpha+\beta)}\sum_n \left(\frac{r}{h}\right)^{S_n}\left[1+\left(\frac{h}{a}\right)^{2S_n}\right]\frac{R\cos(S_n\beta)\sin(S_n\theta)+\sin(S_n\beta)\cos(S_n\theta)}{S_n\sin(S_n\alpha)\cos(S_n\beta)[1+\lambda\cot^2(S_n\alpha)]}$$
$$= \frac{PR}{\mu_1(R\alpha+\beta)}\sum_n \left(\frac{r}{h}\right)^{S_n}\left[1+\left(\frac{h}{a}\right)^{2S_n}\right]\frac{\cos[S_n(\alpha-\theta)]}{S_n\sin^2(S_n\alpha)[1+\lambda\cot^2(S_n\alpha)]}; \quad r \leqslant h$$
$$W_2(r,\theta) = \frac{P}{\mu_1(R\alpha+\beta)}\sum_n \left(\frac{r}{h}\right)^{S_n}\left[1+\left(\frac{h}{a}\right)^{2S_n}\right]\frac{\sin[S_n(\theta+\beta)]}{S_n\sin(S_n\alpha)\cos(S_n\beta)[1+\lambda\cot^2(S_n\alpha)]}; \quad r \leqslant h \tag{16}$$
$$W_1(r,\theta) = \frac{PR}{\mu_1(R\alpha+\beta)}\sum_n \left(\frac{h}{r}\right)^{S_n}\left[1+\left(\frac{r}{a}\right)^{2S_n}\right]\frac{\cos[S_n(\alpha-\theta)]}{S_n\sin^2(S_n\alpha)[1+\lambda\cot^2(S_n\alpha)]}; \quad r \geqslant h$$
$$W_2(r,\theta) = \frac{P}{\mu_1(R\alpha+\beta)}\sum_n \left(\frac{h}{r}\right)^{S_n}\left[1+\left(\frac{r}{a}\right)^{2S_n}\right]\frac{\sin[S_n(\theta+\beta)]}{S_n\sin(S_n\alpha)\cos(S_n\beta)[1+\lambda\cot^2(S_n\alpha)]}; \quad r \geqslant h$$

where

$$\lambda = \frac{R(\alpha+R\beta)}{R\alpha+\beta} \tag{17}$$

and S_n's are the positive roots of the following characteristic equation:

$$R\cos(S_n\alpha)\cos(S_n\beta) - \sin(S_n\alpha)\sin(S_n\beta) = 0 \tag{18}$$

or in a simpler form

$$\tan(S_n\alpha)\tan(S_n\beta) = R \tag{19}$$

Application of Eq. (1) in (16), results in the stress distribution in the composite wedge

$$
\begin{aligned}
\tau_{rz}^{1}(r,\theta) &= \frac{PR}{(R\alpha+\beta)h}\sum_{n}\left(\frac{r}{h}\right)^{S_n-1}\left[1+\left(\frac{h}{a}\right)^{2S_n}\right]\frac{\cos[S_n(\alpha-\theta)]}{\sin^2(S_n\alpha)[1+\lambda\cot^2(S_n\alpha)]}; \quad r\leqslant h\\
\tau_{rz}^{2}(r,\theta) &= \frac{PR}{(R\alpha+\beta)h}\sum_{n}\left(\frac{r}{h}\right)^{S_n-1}\left[1+\left(\frac{h}{a}\right)^{2S_n}\right]\frac{\sin[S_n(\theta+\beta)]}{\sin(S_n\alpha)\cos(S_n\beta)[1+\lambda\cot^2(S_n\alpha)]}; \quad r\leqslant h\\
\tau_{\theta z}^{1}(r,\theta) &= \frac{PR}{(R\alpha+\beta)h}\sum_{n}\left(\frac{r}{h}\right)^{S_n-1}\left[1+\left(\frac{h}{a}\right)^{2S_n}\right]\frac{\sin[S_n(\alpha-\theta)]}{\sin^2(S_n\alpha)[1+\lambda\cot^2(S_n\alpha)]}; \quad r\leqslant h\\
\tau_{\theta z}^{2}(r,\theta) &= \frac{PR}{(R\alpha+\beta)h}\sum_{n}\left(\frac{r}{h}\right)^{S_n-1}\left[1+\left(\frac{h}{a}\right)^{2S_n}\right]\frac{\cos[S_n(\theta+\beta)]}{\sin(S_n\alpha)\cos(S_n\beta)[1+\lambda\cot^2(S_n\alpha)]}; \quad r\leqslant h\\
\tau_{rz}^{1}(r,\theta) &= \frac{PR}{(R\alpha+\beta)h}\sum_{n}\left(\frac{h}{r}\right)^{S_n+1}\left[1-\left(\frac{r}{a}\right)^{2S_n}\right]\frac{\cos[S_n(\alpha-\theta)]}{\sin^2(S_n\alpha)[1+\lambda\cot^2(S_n\alpha)]}; \quad r\geqslant h\\
\tau_{rz}^{2}(r,\theta) &= \frac{PR}{(R\alpha+\beta)h}\sum_{n}\left(\frac{h}{r}\right)^{S_n+1}\left[1-\left(\frac{r}{a}\right)^{2S_n}\right]\frac{\sin[S_n(\theta+\beta)]}{\sin(S_n\alpha)\cos(S_n\beta)[1+\lambda\cot^2(S_n\alpha)]}; \quad r\geqslant h\\
\tau_{\theta z}^{1}(r,\theta) &= \frac{PR}{(R\alpha+\beta)h}\sum_{n}\left(\frac{h}{r}\right)^{S_n+1}\left[1+\left(\frac{r}{a}\right)^{2S_n}\right]\frac{\sin[S_n(\alpha-\theta)]}{\sin^2(S_n\alpha)[1+\lambda\cot^2(S_n\alpha)]}; \quad r\geqslant h\\
\tau_{\theta z}^{2}(r,\theta) &= \frac{PR}{(R\alpha+\beta)h}\sum_{n}\left(\frac{h}{r}\right)^{S_n+1}\left[1+\left(\frac{r}{a}\right)^{2S_n}\right]\frac{\cos[S_n(\theta+\beta)]}{\sin(S_n\alpha)\cos(S_n\beta)[1+\lambda\cot^2(S_n\alpha)]}; \quad r\geqslant h
\end{aligned} \tag{20}
$$

Eqs. (20) show that a stress singularity may occur at the wedge apex which has an order of

$$\lambda_S = 1 - S_1 \tag{21}$$

where S_1 is the least of the poles S_n. Whether or not stress singularity occurs at the apex depends upon the inequality $|S_1| < 1$ holds.

In the special case, when $\beta = 0$ and $\mu_1 = \mu_2 = \mu$, the problem reduces to that of a simple finite wedge and we have from Eq. (18)

$$
\begin{aligned}
W(r,\theta) &= \frac{P}{\mu}\sum_{n=0}^{\infty}(-1)^n\frac{2}{(2n+1)\pi}\left[1+\left(\frac{h}{a}\right)^{\frac{(2n+1)\pi}{\alpha}}\right]\left(\frac{r}{h}\right)^{\frac{(2n+1)\pi}{2\alpha}}\sin\left(\frac{(2n+1)\pi\theta}{2\alpha}\right); \quad r\leqslant h\\
W(r,\theta) &= \frac{P}{\mu}\sum_{n=0}^{\infty}(-1)^n\frac{2}{(2n+1)\pi}\left[1+\left(\frac{r}{a}\right)^{\frac{(2n+1)\pi}{\alpha}}\right]\left(\frac{h}{r}\right)^{\frac{(2n+1)\pi}{2\alpha}}\sin\left(\frac{(2n+1)\pi\theta}{2\alpha}\right); \quad r\geqslant h
\end{aligned} \tag{22}
$$

which is the same as that published by Kargarnovin et al. (1997) for a simple finite isotropic wedge.

In the special case of equal apex angles ($\alpha = \beta$), the characteristic equation (19) reduces to

$$\tan(S_n\alpha) = \pm\sqrt{R} \tag{23}$$

which can be solved to yield

$$
\begin{aligned}
S_n &= \frac{1}{\alpha}\tan^{-1}(\sqrt{R}) + \frac{n\pi}{\alpha}\\
S_n &= \frac{\pi - \tan^{-1}(\sqrt{R})}{\alpha} + \frac{n\pi}{\alpha}; \quad n = 0,1,2,\ldots
\end{aligned} \tag{24}
$$

Selecting the least of the roots $S_1 = \frac{1}{\alpha}\tan^{-1}(\sqrt{R})$, the order of stress singularity appears as

$$\lambda_S = 1 - \frac{1}{\alpha}\tan^{-1}(\sqrt{R}) \tag{25}$$

Eq. (25) shows that the stress singularity is explicitly dependent on the material property. The occurrence of the stress singularity in this case is restricted to the condition:

$$\alpha > \tan^{-1}(\sqrt{R}) \tag{26}$$

This inequality specifies the apex angles for which the stress singularity does occur at the wedge apex. It is noteworthy that the angles for which the singularity occurs at the apex depend on the material property of the bi-material wedge. For example, for similar bonded wedges ($\mu_1 = \mu_2$ or $R = 1$), the apex angles for which the singularity occurs at the apex, are those which are greater than $\frac{\pi}{4}$. However, for $R = \infty$, the singularity occurs in wedges the apex angles of which are greater than $\frac{\pi}{2}$. Hence, for a bi-material wedge with mismatch ratio $R = 1$, a square-root singularity exists at the apex if $\alpha = \frac{\pi}{2}$, however, for a composite wedge with $R = \infty$, the same singularity occurs if $\alpha = \pi$.

2.2.2. Case Ib—traction–traction

The boundary conditions corresponding to this problem are

$$\begin{aligned} &\tau^1_{\theta z}(r,\alpha) = P\delta(r-h)\\ &\tau^2_{\theta z}(r,-\beta) = P\delta(r-h)\\ &W_1(r,0) = W_2(r,0)\\ &\tau^1_{\theta z}(r,0) = \tau^2_{\theta z}(r,0)\end{aligned} \tag{27}$$

Application of the Mellin transform of the second kind, in conjunction with the second of Eq. (1), on the boundary conditions (27) and then, using the resultant relations for obtaining the unknown coefficients of Eq. (12), with $j = 2$, result in

$$\begin{aligned} W^*_{12}(S,\theta) &= \frac{P\left[a^{2S}h^{-S} + h^S\right]\{\cos[S(\alpha-\beta)] - \cos[S(\theta+\beta)] + (R-1)\sin(S\beta)\sin(S\theta)\}}{\mu_1 S[R\cos(S\alpha)\sin(S\beta) + \sin(S\alpha)\cos(S\beta)]}\\ W^*_{22}(S,\theta) &= \frac{P[a^{2S}h^{-S} + h^S]\{\cos[S(\alpha-\beta)] - \cos[S(\theta+\beta)] - \frac{R-1}{R}\sin(S\alpha)\sin(S\theta)\}}{\mu_1 S[R\cos(S\alpha)\sin(S\beta) + \sin(S\alpha)\cos(S\beta)]}\end{aligned} \tag{28}$$

Applying the inversion formula (6) and using the residue theorem for contour integration as explained by Kargarnovin et al. (1997), we obtain

$$\begin{aligned} W_1(r,\theta) &= \frac{P}{\mu_1(R\alpha+\beta)}\sum_n \left(\frac{r}{h}\right)^{S_n}\left[1+\left(\frac{h}{a}\right)^{2S_n}\right]\\ &\quad\times\frac{\cos[S_n(\alpha-\theta)] - \cos[S_n(\theta+\beta)] + (R-1)\sin(S_n\beta)\sin(S_n\theta)}{S_n\sin(S_n\alpha)\sin(S_n\beta)[1+\lambda\cot^2(S_n\alpha)]}; \quad r \leqslant h\\ W_2(r,\theta) &= \frac{P}{\mu_1(R\alpha+\beta)}\sum_n \left(\frac{r}{h}\right)^{S_n}\left[1+\left(\frac{h}{a}\right)^{2S_n}\right]\\ &\quad\times\frac{\cos[S_n(\alpha-\theta)] - \cos[S_n(\theta+\beta)] - \frac{R-1}{R}\sin(S_n\alpha)\sin(S_n\theta)}{S_n\sin(S_n\alpha)\sin(S_n\beta)[1+\lambda\cot^2(S_n\alpha)]}; \quad r \leqslant h\\ W_1(r,\theta) &= \frac{P}{\mu_1(R\alpha+\beta)}\sum_n \left(\frac{h}{r}\right)^{S_n}\left[1+\left(\frac{r}{a}\right)^{2S_n}\right]\\ &\quad\times\frac{\cos[S_n(\alpha-\theta)] - \cos[S_n(\theta+\beta)] + (R-1)\sin(S_n\beta)\sin(S_n\theta)}{S_n\sin(S_n\alpha)\sin(S_n\beta)[1+\lambda\cot^2(S_n\alpha)]}; \quad r \geqslant h\\ W_2(r,\theta) &= \frac{P}{\mu_1(R\alpha+\beta)}\sum_n \left(\frac{h}{r}\right)^{S_n}\left[1+\left(\frac{r}{a}\right)^{2S_n}\right]\\ &\quad\times\frac{\cos[S_n(\alpha-\theta)] - \cos[S_n(\theta+\beta)] - \frac{R-1}{R}\sin(S_n\alpha)\sin(S_n\theta)}{S_n\sin(S_n\alpha)\sin(S_n\beta)[1+\lambda\cot^2(S_n\alpha)]}; \quad r \geqslant h\end{aligned} \tag{29}$$

where λ is defined by the relation (17) and the S_n's are the positive roots of the following characteristic equation:

$$R\cos(S_n\alpha)\sin(S_n\beta) + \sin(S_n\alpha)\cos(S_n\beta) = 0 \tag{30}$$

or in a simpler form

$$\tan(S_n\alpha)\cot(S_n\beta) = -R \tag{31}$$

Now, the stress distribution can be obtained by applying Eq. (1) in Eq. (29), as

$$\begin{aligned}
\tau^1_{rz}(r,\theta) &= \frac{P}{(R\alpha+\beta)h}\sum_n \left(\frac{r}{h}\right)^{S_n-1}\left[1+\left(\frac{h}{a}\right)^{2S_n}\right] \\
&\quad\times \frac{\cos[S_n(\alpha-\theta)] - \cos[S_n(\theta+\beta)] + (R-1)\sin(S_n\beta)\sin(S_n\theta)}{\sin(S_n\alpha)\sin(S_n\beta)[1+\lambda\cot^2(S_n\alpha)]}; \quad r \leqslant h \\
\tau^2_{rz}(r,\theta) &= \frac{PR}{(R\alpha+\beta)h}\sum_n \left(\frac{r}{h}\right)^{S_n-1}\left[1+\left(\frac{h}{a}\right)^{2S_n}\right] \\
&\quad\times \frac{\cos[S_n(\alpha-\theta)] - \cos[S_n(\theta+\beta)] - \frac{R-1}{R}\sin(S_n\alpha)\sin(S_n\theta)}{\sin(S_n\alpha)\sin(S_n\beta)[1+\lambda\cot^2(S_n\alpha)]}; \quad r \leqslant h \\
\tau^1_{\theta z}(r,\theta) &= \frac{P}{(R\alpha+\beta)h}\sum_n \left(\frac{r}{h}\right)^{S_n-1}\left[1+\left(\frac{h}{a}\right)^{2S_n}\right] \\
&\quad\times \frac{\sin[S_n(\alpha-\theta)] + \sin[S_n(\theta+\beta)] + (R-1)\sin(S_n\beta)\cos(S_n\theta)}{\sin(S_n\alpha)\sin(S_n\beta)[1+\lambda\cot^2(S_n\alpha)]}; \quad r \leqslant h \\
\tau^2_{\theta z}(r,\theta) &= \frac{PR}{(R\alpha+\beta)h}\sum_n \left(\frac{r}{h}\right)^{S_n-1}\left[1+\left(\frac{h}{a}\right)^{2S_n}\right] \\
&\quad\times \frac{\sin[S_n(\alpha-\theta)] + \sin[S_n(\theta+\beta)] - \frac{R-1}{R}\sin(S_n\alpha)\cos(S_n\theta)}{\sin(S_n\alpha)\sin(S_n\beta)[1+\lambda\cot^2(S_n\alpha)]}; \quad r \leqslant h \\
\tau^1_{rz}(r,\theta) &= \frac{P}{(R\alpha+\beta)h}\sum_n \left(\frac{h}{r}\right)^{S_n+1}\left[1-\left(\frac{r}{a}\right)^{2S_n}\right] \\
&\quad\times \frac{\cos[S_n(\alpha-\theta)] - \cos[S_n(\theta+\beta)] + (R-1)\sin(S_n\beta)\sin(S_n\theta)}{\sin(S_n\alpha)\sin(S_n\beta)[1+\lambda\cot^2(S_n\alpha)]}; \quad r \geqslant h \\
\tau^2_{rz}(r,\theta) &= \frac{PR}{(R\alpha+\beta)h}\sum_n \left(\frac{h}{r}\right)^{S_n+1}\left[1-\left(\frac{r}{a}\right)^{2S_n}\right] \\
&\quad\times \frac{\cos[S_n(\alpha-\theta)] - \cos[S_n(\theta+\beta)] - \frac{R-1}{R}\sin(S_n\alpha)\sin(S_n\theta)}{\sin(S_n\alpha)\sin(S_n\beta)[1+\lambda\cot^2(S_n\alpha)]}; \quad r \geqslant h \\
\tau^1_{\theta z}(r,\theta) &= \frac{P}{(R\alpha+\beta)h}\sum_n \left(\frac{h}{r}\right)^{S_n+1}\left[1+\left(\frac{r}{a}\right)^{2S_n}\right] \\
&\quad\times \frac{\sin[S_n(\alpha-\theta)] + \sin[S_n(\theta+\beta)] + (R-1)\sin(S_n\beta)\cos(S_n\theta)}{\sin(S_n\alpha)\sin(S_n\beta)[1+\lambda\cot^2(S_n\alpha)]}; \quad r \geqslant h \\
\tau^2_{\theta z}(r,\theta) &= \frac{PR}{(R\alpha+\beta)h}\sum_n \left(\frac{h}{r}\right)^{S_n+1}\left[1+\left(\frac{r}{a}\right)^{2S_n}\right] \\
&\quad\times \frac{\sin[S_n(\alpha-\theta)] + \sin[S_n(\theta+\beta)] - \frac{R-1}{R}\sin(S_n\alpha)\cos(S_n\theta)}{\sin(S_n\alpha)\sin(S_n\beta)[1+\lambda\cot^2(S_n\alpha)]}; \quad r \geqslant h
\end{aligned} \tag{32}$$

Again, a singularity of the order λ_S, as defined in Eq. (21), may occur at the wedge apex, provided that $|S_1| < 1$.

Letting $a \to \infty$ in Eq. (32), the problem reduces to that of two bonded dissimilar wedges with infinite radii. The obtained results in this case are exactly the same as that published by the author (Shahani and Adibnazari, 2000).

In the special case of equal apex angles ($\alpha = \beta$), it is convenient to use Eq. (30) for finding the poles. Applying $\alpha = \beta$ in Eq. (30) gives

$$\sin(S_n\alpha)\cos(S_n\alpha) = 0 \tag{33}$$

which gives two sets of poles

$$S_n = \frac{n\pi}{\alpha}$$
$$S_n = \frac{(2n+1)\pi}{2\alpha}; \quad n = 0, 1, 2, 3, \ldots \tag{34}$$

Replacing these simple poles into Eq. (32), results in after some mathematical manipulations:

$$\begin{aligned}
\tau_{rz}^1(r,\theta) = \tau_{rz}^2(r,\theta) &= \frac{p}{h\alpha}\sum_{n=0}^{\infty}(-1)^n\left(\frac{r}{h}\right)^{\frac{(2n+1)\pi}{2\alpha}-1}\left[1+\left(\frac{h}{a}\right)^{\frac{(2n+1)\pi}{\alpha}}\right]\sin\left(\frac{(2n+1)\pi\theta}{2\alpha}\right); \quad r \leqslant h \\
\tau_{\theta z}^1(r,\theta) = \tau_{\theta z}^2(r,\theta) &= \frac{p}{h\alpha}\sum_{n=0}^{\infty}(-1)^n\left(\frac{r}{h}\right)^{\frac{(2n+1)\pi}{2\alpha}-1}\left[1+\left(\frac{h}{a}\right)^{\frac{(2n+1)\pi}{\alpha}}\right]\cos\left(\frac{(2n+1)\pi\theta}{2\alpha}\right); \quad r \leqslant h \\
\tau_{rz}^1(r,\theta) = \tau_{rz}^2(r,\theta) &= \frac{p}{h\alpha}\sum_{n=0}^{\infty}(-1)^n\left(\frac{h}{r}\right)^{\frac{(2n+1)\pi}{2\alpha}+1}\left[1-\left(\frac{r}{a}\right)^{\frac{(2n+1)\pi}{\alpha}}\right]\sin\left(\frac{(2n+1)\pi\theta}{2\alpha}\right); \quad r \geqslant h \\
\tau_{\theta z}^1(r,\theta) = \tau_{\theta z}^2(r,\theta) &= \frac{p}{h\alpha}\sum_{n=0}^{\infty}(-1)^n\left(\frac{h}{r}\right)^{\frac{(2n+1)\pi}{2\alpha}+1}\left[1+\left(\frac{r}{a}\right)^{\frac{(2n+1)\pi}{\alpha}}\right]\cos\left(\frac{(2n+1)\pi\theta}{2\alpha}\right); \quad r \geqslant h
\end{aligned} \tag{35}$$

It is observed that the obtained stress distribution for the case of equal apex angles is independent of material property and thus, it is the same for the two dissimilar wedges. Eq. (35) also show that the stress field is bounded in a wedge with $0 < \alpha < \frac{\pi}{2}$, whereas in a wedge with $\frac{\pi}{2} < \alpha < \pi$, there exists a stress singularity of the order

$$\lambda_S = 1 - \frac{\pi}{2\alpha} \tag{36}$$

For $\alpha = \pi$, the composite wedge resembles two bonded semi-circles of different materials with an edge crack. It is seen that a familiar square root singularity exists at the crack tip in this case.

2.3. Problem II

Basically the analysis of problem II parallels that of problem I. Therefore, the analysis has been made brief in this problem. In the sequel, two foregoing cases of boundary data on the radial edges of the wedge are taken into account.

2.3.1. Case IIa—traction–displacement

The boundary conditions on the radial edges are denoted by (13). Applying these conditions with the aid of the second of Eq. (1) in (12) with $j = 1$, results in

$$
\begin{aligned}
W_{11}^{*}(S,\theta) &= \frac{P(a^{2S}h^{-S}-h^{S})[R\sin(S\theta)\cos(S\beta)+\cos(S\theta)\sin(S\beta)]}{\mu_1 S[R\cos(S\alpha)\cos(S\beta)-\sin(S\alpha)\sin(S\beta)]} \\
W_{21}^{*}(S,\theta) &= \frac{P(a^{2S}h^{-S}-h^{S})\sin[S(\theta+\beta)]}{\mu_1 S[R\cos(S\alpha)\cos(S\beta)-\sin(S\alpha)\sin(S\beta)]}
\end{aligned}
\tag{37}
$$

Taking the inverse Mellin transform, Eq. (6) with j = 1, and computing the inversion integrals by means of the residue theorem with the same line of calculations explained by Kargarnovin et al. (1997), lead to

$$
\begin{aligned}
W_1(r,\theta) &= \frac{PR}{\mu_1(R\alpha+\beta)}\sum_n \left(\frac{r}{h}\right)^{S_n}\left[1-\left(\frac{h}{a}\right)^{2S_n}\right]\frac{\cos[S_n(\alpha-\theta)]}{S_n\sin^2(S_n\alpha)[1+\lambda\cot^2(S_n\alpha)]}; \quad r\leqslant h \\
W_2(r,\theta) &= \frac{P}{\mu_1(R\alpha+\beta)}\sum_n \left(\frac{r}{h}\right)^{S_n}\left[1-\left(\frac{h}{a}\right)^{2S_n}\right]\frac{\sin[S_n(\theta+\beta)]}{S_n\sin(S_n\alpha)\cos(S_n\beta)[1+\lambda\cot^2(S_n\alpha)]}; \quad r\leqslant h \\
W_1(r,\theta) &= \frac{PR}{\mu_1(R\alpha+\beta)}\sum_n \left(\frac{h}{r}\right)^{S_n}\left[1-\left(\frac{r}{a}\right)^{2S_n}\right]\frac{\cos[S_n(\alpha-\theta)]}{S_n\sin^2(S_n\alpha)[1+\lambda\cot^2(S_n\alpha)]}; \quad r\geqslant h \\
W_2(r,\theta) &= \frac{P}{\mu_1(R\alpha+\beta)}\sum_n \left(\frac{h}{r}\right)^{S_n}\left[1-\left(\frac{r}{a}\right)^{2S_n}\right]\frac{\sin[S_n(\theta+\beta)]}{S_n\sin(S_n\alpha)\cos(S_n\beta)[1+\lambda\cot^2(S_n\alpha)]}; \quad r\geqslant h
\end{aligned}
\tag{38}
$$

where S_n's are the positive nonzero roots of Eq. (18) or Eq. (19). The stress components may then be computed using Eq. (1). Here, only the $\tau_{\theta z}$-component is given in the $r\leqslant h$ region, for the sake of brevity:

$$
\begin{aligned}
\tau_{\theta z}^{1}(r,\theta) &= \frac{PR}{(R\alpha+\beta)h}\sum_n \left(\frac{r}{h}\right)^{S_n-1}\left[1-\left(\frac{h}{a}\right)^{2S_n}\right]\frac{\sin[S_n(\alpha-\theta)]}{\sin^2(S_n\alpha)[1+\lambda\cot^2(S_n\alpha)]}; \quad r\leqslant h \\
\tau_{\theta z}^{2}(r,\theta) &= \frac{PR}{(R\alpha+\beta)h}\sum_n \left(\frac{r}{h}\right)^{S_n-1}\left[1-\left(\frac{h}{a}\right)^{2S_n}\right]\frac{\cos[S_n(\theta+\beta)]}{\sin(S_n\alpha)\cos(S_n\beta)[1+\lambda\cot^2(S_n\alpha)]}; \quad r\leqslant h
\end{aligned}
\tag{39}
$$

Turning our attention to a wedge with infinite radius, it is obvious that since at infinity the displacement and stress fields tend to zero, this case should convert to case I a. To verify the statement, it suffices to let $a\to\infty$ in (38) and (39) which reproduces Eqs. (16) and (20).

2.3.2. Case IIb—traction–traction

In a manner similar to case Ib, we take the Mellin transform of the first kind of the boundary conditions (27) and use the results to compute the coefficients in (12) with $j = 1$. The transformed displacements are then

$$
\begin{aligned}
W_{11}^{*}(S,\theta) &= \frac{P\left[a^{2S}h^{-S}-h^{-S}\right]\{\cos[S(\alpha-\beta)]-\cos[S(\theta+\beta)]+(R-1)\sin(S\beta)\sin(S\theta)\}}{\mu_1 S[R\cos(S\alpha)\sin(S\beta)+\sin(S\alpha)\cos(S\beta)]} \\
W_{21}^{*}(S,\theta) &= \frac{P\left[a^{2S}h^{-S}-h^{S}\right]\{\cos[S(\alpha-\beta)]-\cos[S(\theta+\beta)]-\frac{R-1}{R}\sin(S\alpha)\sin(S\theta)\}}{\mu_1 S[R\cos(S\alpha)\sin(S\beta)+\sin(S\alpha)\cos(S\beta)]}
\end{aligned}
\tag{40}
$$

Taking the inverse Mellin transform using Eq. (6) with $j = 1$, leads to

$$
\begin{aligned}
W_1(r,\theta) &= \frac{P}{\mu_1(R\alpha+\beta)}\sum_n\left(\frac{r}{h}\right)^{S_n}\left[1-\left(\frac{h}{a}\right)^{2S_n}\right] \\
&\quad\times\frac{\cos[S_n(\alpha-\theta)]-\cos[S_n(\theta+\beta)]+(R-1)\sin(S_n\beta)\sin(S_n\theta)}{S_n\sin(S_n\alpha)\sin(S_n\beta)[1+\lambda\cot^2(S_n\alpha)]};\quad r\leqslant h \\
W_2(r,\theta) &= \frac{P}{\mu_1(R\alpha+\beta)}\sum_n\left(\frac{r}{h}\right)^{S_n}\left[1-\left(\frac{h}{a}\right)^{2S_n}\right] \\
&\quad\times\frac{\cos[S_n(\alpha-\theta)]-\cos[S_n(\theta+\beta)]-\frac{R-1}{R}\sin(S_n\alpha)\sin(S_n\theta)}{S_n\sin(S_n\alpha)\sin(S_n\beta)[1+\lambda\cot^2(S_n\alpha)]};\quad r\leqslant h \\
W_1(r,\theta) &= \frac{P}{\mu_1(R\alpha+\beta)}\sum_n\left(\frac{h}{r}\right)^{S_n}\left[1-\left(\frac{r}{a}\right)^{2S_n}\right] \\
&\quad\times\frac{\cos[S_n(\alpha-\theta)]-\cos[S_n(\theta+\beta)]+(R-1)\sin(S_n\beta)\sin(S_n\theta)}{S_n\sin(S_n\alpha)\sin(S_n\beta)[1+\lambda\cot^2(S_n\alpha)]};\quad r\geqslant h \\
W_2(r,\theta) &= \frac{P}{\mu_1(R\alpha+\beta)}\sum_n\left(\frac{h}{r}\right)^{S_n}\left[1-\left(\frac{r}{a}\right)^{2S_n}\right] \\
&\quad\times\frac{\cos[S_n(\alpha-\theta)]-\cos[S_n(\theta+\beta)]-\frac{R-1}{R}\sin(S_n\alpha)\sin(S_n\theta)}{S_n\sin(S_n\alpha)\sin(S_n\beta)[1+\lambda\cot^2(S_n\alpha)]};\quad r\geqslant h
\end{aligned}
\tag{41}
$$

where S_n's are the positive nonzero roots of Eq. (30) or Eq. (31). The stress components can then be computed using Eq. (1), of which only the $\tau_{\theta z}$-component is given here

$$
\begin{aligned}
\tau^1_{\theta z}(r,\theta) &= \frac{P}{(R\alpha+\beta)h}\sum_n\left(\frac{r}{h}\right)^{S_n-1}\left[1-\left(\frac{h}{a}\right)^{2S_n}\right] \\
&\quad\times\frac{\sin[S_n(\alpha-\theta)]+\sin[S_n(\theta+\beta)]+(R-1)\sin(S_n\beta)\cos(S_n\theta)}{\sin(S_n\alpha)\sin(S_n\beta)[1+\lambda\cot^2(S_n\alpha)]};\quad r\leqslant h \\
\tau^2_{\theta z}(r,\theta) &= \frac{PR}{(R\alpha+\beta)h}\sum_n\left(\frac{r}{h}\right)^{S_n-1}\left[1-\left(\frac{h}{a}\right)^{2S_n}\right] \\
&\quad\times\frac{\sin[S_n(\alpha-\theta)]+\sin[S_n(\theta+\beta)]-\frac{R-1}{R}\sin(S_n\alpha)\cos(S_n\theta)}{\sin(S_n\alpha)\sin(S_n\beta)[1+\lambda\cot^2(S_n\alpha)]};\quad r\leqslant h
\end{aligned}
\tag{42}
$$

Letting $a \to \infty$ in Eqs. (29), (32) and (41), (42), we arrive in the same relations for the bonded wedges with infinite radii, the results which accord with that published by Shahani and Adibnazari (2000).

For the special case of equal apex angles ($\alpha = \beta$), Eq. (42) reduce to

$$
\tau^1_{\theta z}(r,\theta)=\tau^2_{\theta z}(r,\theta)=\frac{p}{h\alpha}\sum_{n=0}^{\infty}(-1)^n\left(\frac{r}{h}\right)^{\frac{(2n+1)\pi}{2\alpha}-1}\left[1-\left(\frac{h}{a}\right)^{\frac{(2n+1)\pi}{\alpha}}\right]\cos\left(\frac{(2n+1)\pi\theta}{2\alpha}\right);\quad r\leqslant h \tag{43}
$$

3. Part II: mode III stress intensity factor in bi-material media containing an interfacial edge crack

In part II, we are going to use the results of part I and derive the stress intensity factors at the tip of an interfacial edge crack in bi-material circular media. Indeed, the geometry under consideration is the special case of two bonded dissimilar finite wedges, whose apex angles are such that they form a circular bi-material shaft containing an interfacial edge crack, i.e., $\alpha + \beta = 2\pi$, as shown in Fig. 2.

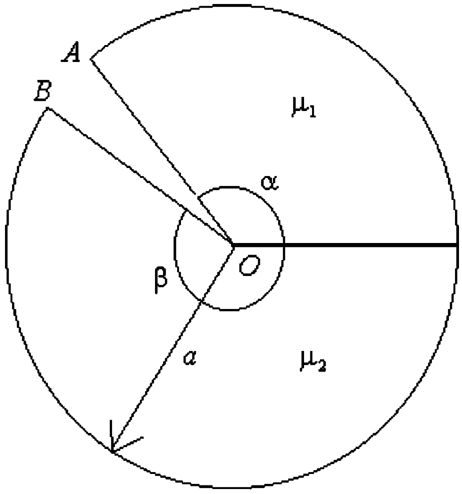

Fig. 2. Schematic view of a bi-material circular media containing an interfacial edge crack.

The radial edges of the composite wedge (the crack faces in this special case), can be subjected both to tractions (traction–traction) or one be fixed and the other subjected to traction (traction–displacement), as explained in part I. Here, it is considered that the crack face OA is subjected to concentrated traction perpendicular to the plane of Fig. 1 in the outward direction with a distance h from the crack tip. However, the edge OB either is subjected to concentrated traction perpendicular to the plane of Fig. 1 in the inward direction at a distance h from the crack tip in the traction–traction case, or is fixed in the traction–displacement case.

Without loss of generality, we assume $\beta \geqslant \alpha$. The stress intensity factor at the crack tip can be computed using the following formula:

$$K_{\mathrm{III}} = \lim_{r\to 0} \sqrt{2\pi} r^{\lambda_S} \tau^2_{\theta z}(r, \alpha - \pi) \tag{44}$$

where λ_S is the order of stress singularity at the wedge apex (the crack tip in this case), as defined in part I of this paper. Using the expressions obtained for the stress components in part I, the stress intensity factor can be computed with the aid of Eq. (44). This is done here for the two different problems described in part I, i.e., bi-material wedge with traction free boundary condition prescribed on the circular segment (problem I) and bi-material wedge fixed on the circular segment (problem II).

3.1. Problem I

3.1.1. Case Ia—traction–displacement

$$K_{\mathrm{III}} = \frac{\sqrt{2\pi}PR}{(R\alpha+\beta)h^{S_1}} \frac{\left[1+\left(\frac{h}{a}\right)^{2S_1}\right]\cos(\pi S_1)}{\sin(S_1\alpha)\cos(S_1\beta)[1+\lambda\cot^2(S_1\alpha)]} \tag{45}$$

where S_1 is the least positive (nonzero) root of the characteristic equation (18) or (19).

3.1.2. Case Ib—traction–traction

$$K_{\mathrm{III}} = \frac{\sqrt{2\pi}PR}{(R\alpha+\beta)h^{S_1}} \frac{\left[1+\left(\frac{h}{a}\right)^{2S_1}\right]\left\{2\sin(S_1\pi) - \frac{R-1}{R}\sin(S_1\alpha)\cos[S_1(\alpha-\pi)]\right\}}{\sin(S_1\alpha)\sin(S_1\beta)[1+\lambda\cot^2(S_1\alpha)]} \tag{46}$$

where S_1 is the least positive (nonzero) root of the characteristic equation (30) or (31).

3.2. Problem II

3.2.1. Case IIa—traction–displacement

$$K_{\mathrm{III}} = \frac{\sqrt{2\pi}PR}{(R\alpha + \beta)h^{S_1}} \frac{\left[1 - \left(\frac{h}{a}\right)^{2S_1}\right]\cos(S_1\pi)}{\sin(S_1\alpha)\cos(S_1\beta)[1 + \lambda\cot^2(S_1\alpha)]} \tag{47}$$

where S_1 is the least positive (nonzero) root of the characteristic equation (18) or (19).

3.2.2. Case IIb—traction–traction

$$K_{\mathrm{III}} = \frac{\sqrt{2\pi}PR}{(R\alpha + \beta)h^{S_1}} \frac{\left[1 - \left(\frac{h}{a}\right)^{2S_1}\right]\left\{2\sin(S_1\pi) - \frac{R-1}{R}\sin(S_1\alpha)\cos[S_1(\alpha - \pi)]\right\}}{\sin(S_1\alpha)\sin(S_1\beta)[1 + \lambda\cot^2(S_1\alpha)]} \tag{48}$$

where S_1 is the least positive (nonzero) root of the characteristic equation (30) or (31).

4. Special case of bonded wedges with similar materials

In this case $\mu_1 = \mu_2$ or $R = 1$ and the twin problems are considered here separately.

4.1. Problem I

4.1.1. Case Ia—traction–displacement

Substitution of $R = 1$ into the corresponding characteristic equation (Eq. (19)), yields

$$\tan(S_n\alpha)\tan(S_n\beta) = 1$$

or

$$\tan(S_n\alpha) = \cot(S_n\beta) = \tan\left(\frac{\pi}{2} - S_n\beta\right)$$

which gives

$$S_n = \frac{(2n+1)\pi}{2(\alpha + \beta)}; \quad n = 0, 1, 2, \ldots \tag{49}$$

For the considered interfacial crack problem, $\alpha + \beta = 2\pi$ and thus, it can be concluded from Eq. (49)

$$S_n = \frac{2n+1}{4}; \quad n = 0, 1, 2, \ldots \tag{50}$$

Choosing the least positive value of the roots, we have

$$S_1 = \frac{1}{4} \tag{51}$$

Substituting this into Eq. (45) and facilitating terms, lead to

$$K_{\mathrm{III}} = \frac{P}{2\sqrt{\pi}h^{\frac{1}{4}}}\left[1 + \left(\frac{h}{a}\right)^{\frac{1}{2}}\right] \tag{52}$$

It is observed that in the case of similar materials, the result becomes independent of the effect of the selection of apex angles. This agrees with the physical nature of the problem, since in this case the problem reduces to that of a circular shaft with an edge crack. The same result as Eq. (52) can be obtained from the analysis of a simple isotropic wedge with finite radius as accomplished by Kargarnovin et al. (1997), letting $\alpha = 2\pi$ and using Eq. (44). It is seen that for an infinite space ($a \to \infty$), the stress intensity factor becomes

$$K_{\mathrm{III}} = \frac{P}{2\sqrt{\pi}h^{\frac{1}{4}}} \tag{53}$$

Also, for a finite shaft the stress intensity factor varies from $\frac{P}{\sqrt{\pi}a^{1/4}}$ for $h = a$ to infinity when the concentrated traction is applied at the crack tip ($h = 0$).

4.1.2. Case Ib—traction–traction

Replacing $R = 1$ in the corresponding characteristic equation (Eq. (31)), leads to

$$\tan(S_n\alpha)\cot(S_n\beta) = -1$$

or

$$\tan(S_n\alpha) = -\tan(S_n\beta)$$

which gives

$$S_n = \frac{n\pi}{\alpha+\beta}; \quad n = 0, 1, 2, \ldots \tag{54}$$

For the interfacial crack problem, $\alpha + \beta = 2\pi$ and hence, we have

$$S_n = \frac{n}{2}; \quad n = 0, 1, 2, \ldots \tag{55}$$

Selecting the least positive value of the roots, results in

$$S_1 = \frac{1}{2} \tag{56}$$

Substituting into Eq. (46) gives after some mathematical manipulations

$$K_{\mathrm{III}} = \frac{\sqrt{2}P}{\sqrt{\pi h}}\left(1 + \frac{h}{a}\right) \tag{57}$$

This result is the same as that published recently by the author (Shahani, 2003) for a simple isotropic circular shaft with an edge crack under the same loading.

It is seen that the stress intensity factor varies from $\frac{2\sqrt{2}P}{\sqrt{\pi\alpha}}$ when $h = a$, to infinity when the concentrated traction coincides with the crack tip ($h = 0$). Also, for an infinite space with an edge crack ($a \to \infty$), we have

$$K_{\mathrm{III}} = \frac{\sqrt{2}P}{\sqrt{\pi h}} \tag{58}$$

4.2. Problem II

4.2.1. Case IIa—traction–displacement

Again, for bonded wedges of similar materials in this case, the poles are given with Eqs. (50) and (51) for the least of the poles. Computing the stress intensity factor results in

$$K_{\mathrm{III}} = \frac{P}{2\sqrt{\pi}h^{\frac{1}{4}}}\left[1 - \left(\frac{h}{a}\right)^{\frac{1}{2}}\right] \tag{59}$$

It is seen that the stress intensity factor varies from zero when $h = a$, to infinity when the concentrated traction is applied at the crack tip ($h = 0$).

Turning our attention to an infinite space with an edge crack, it is obvious that since at infinity the displacement and stress fields tend to zero, this case should convert to case Ia. To verify the statement suffice to let $a \to \infty$ in (59) and reproduce (53).

4.2.2. Case IIb—traction–traction

In this case, the equation of the poles is the same Eq. (55) and S_1 is given by Eq. (56). Thus, the stress intensity factor can be computed as

$$K_{\text{III}} = \frac{\sqrt{2}P}{\sqrt{\pi h}}\left(1 - \frac{h}{a}\right) \tag{60}$$

It is noteworthy that the stress intensity factor varies from zero for $h = a$, to infinity in the case of coincidence of the concentrated traction with the crack tip ($h = 0$). Again, in the special case of infinite space with an edge crack $a \to \infty$, the same result as the case Ib is obtained (Eq. (58)).

5. Various combinations of the apex angles of the composite wedge

Here, three combinations of the apex angles are considered which are $\alpha = \beta$, $\beta = 2\alpha$, $\beta = 3\alpha$. In these cases, the corresponding characteristic equations can be solved analytically, which causes that the simplified relations for the stress intensity factors to be obtained.

5.1. The case when $\alpha = \beta$

5.1.1. Problem I

5.1.1.1. Case Ia—traction–displacement. Applying $\alpha = \beta$ into Eq. (19), results in

$$\tan^2(S_n\alpha) = R \tag{61}$$

Eq. (61) can be solved to give

$$S_n = \pm\frac{1}{\alpha}\tan^{-1}(\sqrt{R}) + \frac{n\pi}{\alpha}; \quad n = 0, 1, 2, \ldots \tag{62}$$

Choosing the least positive pole, we have

$$S_1 = \frac{1}{\alpha}\tan^{-1}(\sqrt{R}) \tag{63}$$

Since, $\alpha + \beta = 2\pi$ in the problem considered, then we should have $\alpha = \beta = \pi$. Substituting this and Eq. (63) into Eq. (45), leads to the following expression for the stress intensity factor:

$$K_{\text{III}} = \frac{P}{\sqrt{2\pi}h^{S_1}}\sqrt{\frac{R}{R+1}}\left[1 + \left(\frac{h}{a}\right)^{2S_1}\right] \tag{64}$$

where

$$S_1 = \frac{1}{\pi}\tan^{-1}(\sqrt{R}) \tag{65}$$

It is seen that the stress intensity factor for the bi-material considered, is a function of the material property (R).

5.1.1.2. Case Ib—traction–traction. Applying $\alpha = \beta = \pi$ into Eq. (30), yields

$$\sin(S_n\pi) = 0 \Rightarrow S_n = n; \quad n = 1, 2, 3, \ldots$$

$$\cos(S_n\pi) = 0 \Rightarrow S_n = n + \frac{1}{2}; \quad n = 0, 1, 2, \ldots \tag{66}$$

Choosing the least positive root, $S_1 = \frac{1}{2}$, Eq. (46) reduces to

$$K_{\mathrm{III}} = \frac{\sqrt{2}P}{\sqrt{\pi h}}\left(1 + \frac{h}{a}\right) \tag{67}$$

It is seen that in this case the stress intensity factor is independent of material property. This result could also be obtained directly from Eq. (35) for the special case of equal apex angles, by applying Eq. (44) and $\alpha = \pi$. Because of independency of Eq. (67) of the material property, it is evident that this result must be the same as that obtained for the case of similar materials (Eq. (57)).

5.1.2. Problem II

5.1.2.1. Case IIa—traction–displacement. In this case, we encounter to the same singularity as the case I a (see Eq. (65)) and it can be shown similarly that the stress intensity factor is as follows:

$$K_{\mathrm{III}} = \frac{P}{\sqrt{2\pi}h^{S_1}}\sqrt{\frac{R}{R+1}}\left[1 - \left(\frac{h}{a}\right)^{2S_1}\right] \tag{68}$$

where S_1 is given by Eq. (65). It is noticeable that the stress intensity factor varies from zero for $h = a$, to infinity when $h = 0$. Again, for an infinite composite space with an interfacial crack, the results of the cases Ia and IIa would become the same, i.e.,

$$K_{\mathrm{III}} = \frac{P}{\sqrt{2\pi}h^{S_1}}\sqrt{\frac{R}{R+1}}$$

5.1.2.2. Case IIb—traction–traction. Similar to what followed in the case Ib, the stress intensity factor appears as

$$K_{\mathrm{III}} = \frac{\sqrt{2}P}{\sqrt{\pi h}}\left(1 - \frac{h}{a}\right) \tag{69}$$

In the special case of $a \to \infty$, Eqs. (67) and (69) become coincident.

5.2. The case when $\beta = 2\alpha$

The above relation together with the relation $\alpha + \beta = 2\pi$, result in $\alpha = \frac{2\pi}{3}$ and $\beta = \frac{4\pi}{3}$.

5.2.1. Problem I

5.2.1.1. Case Ia—traction–displacement. Letting

$$x_n = S_n\alpha \tag{70}$$

the characteristic equation corresponding to this case, i.e., Eq. (19) gives

$$\tan x_n \tan 2x_n = \tan x_n \frac{2\tan x_n}{1 - \tan^2 x_n} = R \tag{71}$$

or

$$\tan^2 x_n = \frac{R}{R+2} \Rightarrow x_n = \pm\tan^{-1}\left(\sqrt{\frac{R}{R+2}}\right) + n\pi; \quad n = 0, 1, 2, \ldots \tag{72}$$

Selection of the least positive (nonzero) value of the roots yields

$$S_1 = \frac{1}{\alpha}\tan^{-1}\left(\sqrt{\frac{R}{R+2}}\right) = \frac{3}{2\pi}\tan^{-1}\left(\sqrt{\frac{R}{R+2}}\right) \tag{73}$$

Substituting for S_1 into Eq. (45) yields after some mathematical manipulations:

$$K_{\mathrm{III}} = \frac{3P}{2\sqrt{2\pi}h^{S_1}}\left[1 + \left(\frac{h}{a}\right)^{2S_1}\right]\frac{\sqrt{R(R+1)}}{R+2}\left[1 + 2\frac{R+2}{R+1}\sqrt{\frac{R+2}{2(R+1)}} - 3\sqrt{\frac{R+2}{2(R+1)}}\right]^{\frac{1}{2}} \tag{74}$$

It should be noticed that the stress intensity factor depends upon the material property for the considered bi-material circular shaft. In the special case of $R = 1$, Eq. (74) reduces to Eq. (52).

5.2.1.2. Case Ib—traction–traction. In this case, the characteristic equation (31) can be written as

$$\tan x_n = -R\tan 2x_n = -R\frac{2\tan x_n}{1 - \tan^2 x_n} \tag{75}$$

from which we obtain

$$\tan x_n = 0 \Rightarrow x_n = n\pi$$

$$\tan^2 x_n = 1 + 2R \Rightarrow x_n = \pm\tan^{-1}(\sqrt{1+2R}) + n\pi; \quad n = 0, 1, 2, \ldots \tag{76}$$

Choosing the least positive (nonzero) value of the roots, yields

$$S_1 = \frac{1}{\alpha}\tan^{-1}(\sqrt{1+2R}) = \frac{3}{2\pi}\tan^{-1}(\sqrt{1+2R}) \tag{77}$$

Substitution of S_1 into Eq. (46) and facilitating lead to

$$K_{\mathrm{III}} = \frac{3P\left[1 + \left(\frac{h}{a}\right)^{2S_1}\right]}{2\sqrt{\pi}h^{S_1}} \times \frac{R\sqrt{R+1}}{R+1}\left[\sqrt{2}\sqrt{1 - \frac{2}{(R+1)\sqrt{2(R+1)}} + \frac{3}{\sqrt{2(R+1)}}} - \frac{R-1}{R}\sqrt{\frac{2R+1}{2(R+1)}}\sqrt{\frac{1+\sqrt{2(R+1)}}{2\sqrt{2(R+1)}}}\right] \tag{78}$$

In the special case of a single-material circular shaft with an edge crack ($R = 1$), the same result as Eq. (57) is obtained.

5.2.2. Problem II

5.2.2.1. Case IIa—traction–displacement. In a manner similar to case I a, it can be shown that the stress intensity factor is given by the following relation:

$$K_{\mathrm{III}} = \frac{3P}{2\sqrt{2\pi}h^{S_1}}\left[1 - \left(\frac{h}{a}\right)^{2S_1}\right]\frac{\sqrt{R(R+1)}}{R+2}\left[1 + 2\frac{R+2}{R+1}\sqrt{\frac{R+2}{2(R+1)}} - 3\sqrt{\frac{R+2}{2(R+1)}}\right]^{\frac{1}{2}} \tag{79}$$

where S_1 should be computed from Eq. (73).

5.2.2.2. Case IIb—traction–traction. Following the same line of calculations as case Ib, the stress intensity factor can be obtained as

$$K_{\rm III} = \frac{3P\left[1-\left(\frac{h}{a}\right)^{2S_1}\right]}{2\sqrt{\pi}h^{S_1}} \times \frac{R\sqrt{R+1}}{R+1}\left[\sqrt{2}\sqrt{1-\frac{2}{(R+1)\sqrt{2(R+1)}}+\frac{3}{\sqrt{2(R+1)}}}-\frac{R-1}{R}\sqrt{\frac{2R+1}{2(R+1)}}\sqrt{\frac{1+\sqrt{2(R+1)}}{2\sqrt{2(R+1)}}}\right] \quad (80)$$

where S_1 is given by Eq. (77).

5.3. The case when $\beta = 3\alpha$

The above relation together with $\alpha+\beta=2\pi$ gives $\alpha=\frac{\pi}{2}$ and $\beta=\frac{3\pi}{2}$.

5.3.1. Problem I

5.3.1.1. Case Ia—traction–displacement. The characteristic equation (19) can be written, in this case, as

$$\tan x_n \tan(3x_n) = \tan x_n \frac{3\tan x_n - \tan^3 x_n}{1-3\tan^2 x_n} = R \quad (81)$$

Eq. (81) can be solved to give

$$x_n = \pm\tan^{-1}\left[\frac{1}{\sqrt{2}}\sqrt{3(R+1)\pm\sqrt{9(R+1)^2-4R}}\right]+n\pi; \quad n=0,1,2,\ldots \quad (82)$$

Then, S_1 appears to be

$$S_1 = \frac{2}{\pi}\tan^{-1}\left[\frac{1}{\sqrt{2}}\sqrt{3(R+1)-\sqrt{9(R+1)^2-4R}}\right] \quad (83)$$

Replacing S_1 into Eq. (45) yields after some mathematical manipulations:

$$K_{\rm III} = \frac{4P\left[1+\left(\frac{h}{a}\right)^{2S_1}\right]}{\sqrt{\pi}h^{S_1}} \times \frac{R\left[1-\frac{1}{4}\left(3(R+1)-\sqrt{9(R+1)^2-4R}\right)^2\right]\sqrt{3(R+1)-\sqrt{9(R+1)^2-4R}}}{\left[1-\frac{3}{2}\left(3(R+1)-\sqrt{9(R+1)^2-4R}\right)\right]\left[3(R+1)(R+3)+2R(1+3R)-(R+3)\sqrt{9(R+1)^2-4R}\right]} \quad (84)$$

5.3.1.2. Case Ib—traction–traction. Substituting $\beta = 3\alpha$ into Eq. (31), results in

$$\tan x_n = -R\tan(3x_n) = -R\frac{3\tan x_n - \tan^3 x_n}{1-3\tan^2 x_n} \quad (85)$$

Facilitating terms, we obtain

$$\tan x_n = 0 \Rightarrow x_n = n\pi$$

$$\tan^2 x_n = \frac{1+3R}{3+R} \Rightarrow x_n = \pm\tan^{-1}\left(\sqrt{\frac{1+3R}{3+R}}\right) + n\pi; \quad n = 0, 1, 2, \ldots \tag{86}$$

Choosing the least positive (nonzero) value of the roots, we have

$$S_1 = \frac{1}{\alpha}\tan^{-1}\left(\sqrt{\frac{1+3R}{3+R}}\right) = \frac{2}{\pi}\tan^{-1}\left(\sqrt{\frac{1+3R}{3+R}}\right) \tag{87}$$

Replacing S_1 into Eq. (46) and accomplishing some mathematical operations, we arrive at

$$K_{\mathrm{III}} = \frac{\sqrt{2}P}{\sqrt{\pi}h^{S_1}}\sqrt{\frac{1+3R}{3+R}}\left[1 + \left(\frac{h}{a}\right)^{2S_1}\right] \tag{88}$$

It is easily seen that in the case of a simple isotropic circular shaft containing an edge crack ($R = 1$), Eq. (88) coincides with Eq. (57).

5.3.2. Problem II

5.3.2.1. Case II a—traction–displacement. The stress intensity factor in this case is as follows:

$$K_{\mathrm{III}} = \frac{4P\left[1 - \left(\frac{h}{a}\right)^{2S_1}\right]}{\sqrt{\pi}h^{S_1}} \times \frac{R\left[1 - \frac{1}{4}\left(3(R+1) - \sqrt{9(R+1)^2 - 4R}\right)^2\right]\sqrt{3(R+1) - \sqrt{9(R+1)^2 - 4R}}}{\left[1 - \frac{3}{2}\left(3(R+1) - \sqrt{9(R+1)^2 - 4R}\right)\right]\left[3(R+1)(R+3) + 2R(1+3R) - (R+3)\sqrt{9(R+1)^2 - 4R}\right]} \tag{89}$$

5.3.2.2. Case IIb—traction–traction. The stress intensity factor corresponding to this case appears to be

$$K_{\mathrm{III}} = \frac{\sqrt{2}P}{\sqrt{\pi}h^{S_1}}\sqrt{\frac{1+3R}{3+R}}\left[1 - \left(\frac{h}{a}\right)^{2S_1}\right] \tag{90}$$

References

Bogy, D.B., 1971. Two edge-bonded elastic wedges of different materials and wedge angles under surface tractions. Transaction of ASME, Journal of Applied Mechanics 38, 377–386.

Choi, S.R., Chong, C.H., Chai, Y.S., 1994. Interfacial edge crack in two bonded dissimilar orthotropic quarter planes under antiplane shear. International Journal of Fracture 67, 143–150.

Dempsey, J.P., Sinclair, G.B., 1979. On the stress singularities in the plane elasticity of the composite wedge. Journal of Elasticity 9, 373–391.

Dempsey, J.P., Sinclair, G.B., 1981. On the stress behaviour at the vertex of a bi-material wedge. Journal of Elasticity 11, 317–327.

Fariborz, S.J., 2004. Closure on "Analysis of an isotropic finite wedge under antiplane deformation". International Journal of Solids and Structures 41 (18–19), 5447–5448.

Kargarnovin, M.H., Fariborz, S.J., 2000. Analysis of a dissimilar finite wedge under antiplane deformation. Mechanics Research Communications 27 (1), 109–116.

Kargarnovin, M.H., Shahani, A.R., Fariborz, S.J., 1997. Analysis of an isotropic finite wedge under antiplane deformation. International Journal of Solids and Structures 34, 113–128.

Lee, K.W., Earmme, Y.Y., 2000. An interfacial edge crack in anisotropic bi-material under antiplane singularity. International Journal of Fracture 104, 13–22.

Ma, C.C., Hour, B.L., 1989. Analysis of dissimilar anisotropic wedges subjected to antiplane shear deformation. International Journal of Solids and Structures 25, 1295–1309.

Shahani, A.R., 1999. Analysis of an anisotropic finite wedge under antiplane deformation. Journal of Elasticity 56, 17–32.

Shahani, A.R., Adibnazari, S., 2000. Analysis of perfectly bonded wedges and bonded wedges with an interfacial crack under antiplane shear loading. International Journal of Solids and Structures 37, 2639–2650.

Shahani, A.R., 2001. A note on the paper "Analysis of perfectly bonded wedges and bonded wedges with an interfacial crack under antiplane shear loading". International Journal of Solids and Structures 38, 5041–5043.

Shahani, A.R., 2003. Mode III stress intensity factors for edge-cracked circular shafts, bonded wedges, bonded half planes and DCB's. International Journal of Solids and Structures 40, 6567–6576.

Shahani, A.R., 2004. On the antiplane shear deformation of finite wedges. International Journal of Solids and Structures, Submitted for publication.

Shiue, S.T., Hu, C.T., Lee, S., 1989. Elastic interaction between screw dislocations and a welded surface crack in composite materials. Engineering Fracture Mechanics 33 (5), 697–706.

Sneddon, I.N., 1972. The Use of Integral Transforms. McGraw-Hill Book Co., New York.

Suo, Z., 1989. Singularities Interacting with interfaces and cracks. International Journal of Solids and Structures 25 (10), 1133–1142.

Ting, T.C.T., 1986. Explicit solution and invariance of the singularities at an interface crack in anisotropic composites. International Journal of Solids and Structures 22, 965–983.